

Measurement of temperature-dependent specific heat of biological tissues

Dieter Haemmerich¹, David J Schutt², Icaro dos Santos³,
John G Webster² and David M Mahvi⁴

¹ Division of Pediatric Cardiology, Medical University of South Carolina, 165 Ashley Ave, Charleston, SC 29425, USA

² Department of Biomedical Engineering, University of Wisconsin-Madison, 1550 Engineering Drive, Madison, WI 53706, USA

³ Department of Electrical Engineering, University of Brasilia, Brasilia DF, 70.919-970, Brazil

⁴ Department of Surgery, University of Wisconsin-Madison, 600 Highland Avenue, Madison, WI 53792, USA

E-mail: webster@engr.wisc.edu

Received 8 July 2004, accepted for publication 1 December 2004

Published 10 January 2005

Online at stacks.iop.org/PM/26/59

Abstract

We measured specific heat directly by heating a sample uniformly between two electrodes by an electric generator. We minimized heat loss by styrofoam insulation. We measured temperature from multiple thermocouples at temperatures from 25 °C to 80 °C while heating the sample, and corrected for heat loss. We confirm method accuracy with a 2.5% agar–0.4% saline physical model and obtain specific heat of $4121 \pm 89 \text{ J (kg K)}^{-1}$, with an average error of 3.1%.

Keywords: specific heat, measurement of specific heat, tissue specific heat measurement

1. Introduction

This paper presents a method to measure temperature-dependent specific heat of tissues. Knowledge of temperature-dependent specific heat is required when investigating thermal therapies (e.g., thermal tumor treatment) and other biological heat transfer problems. Data on specific heat of different tissue types are available (Duck 1990, Rahman 1995), though few studies evaluate the specific heat at temperatures above 50 °C. A number of different methods for measuring specific heat are available (Touloukian and Buyco 1970). Differential scanning calorimetry (DSC) is the most practical tool to measure temperature-dependent specific heat of biological materials (Mohesnin 1980, Sweat 1986). DSC requires small samples (millimeter thickness), since uniform sample temperature must be guaranteed. In small samples however,

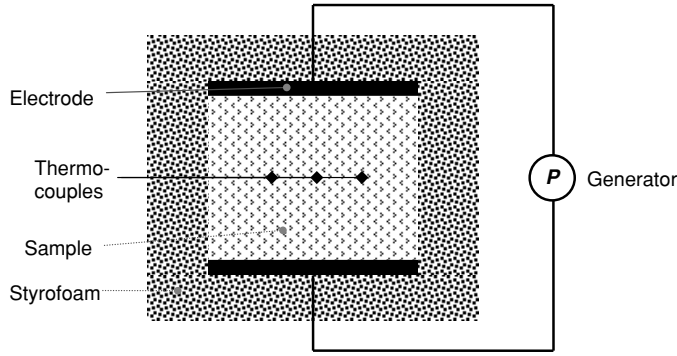


Figure 1. Experimental set-up (side view): A sample ($5 \times 5 \text{ cm}^2$, 4 cm thick) is placed between two metal electrodes. The sample is heated with constant power supplied by a generator, and thermally insulated by 1 cm thick expanded polystyrene. Sample temperature is monitored by six thermocouples.

water bound in the tissue may evaporate markedly below the boiling temperature of water (Ramachandran *et al* 1996), depending on how tight the sealing of the sample is. A previous study reports an increase of heat flow during DSC of liver tissue (which is directly correlated to specific heat) of ~ 5 times at 80°C compared to values below 70°C due to water vaporization from the sample (Ramachandran *et al* 1996). Different seal conditions produce different results when DSC is used and especially at higher temperatures errors can be introduced (Tang *et al* 1991). It may therefore be difficult to choose the seal condition that corresponds to an *in vivo* setting where tissue is heated inside a solid organ.

We present a simple method that allows measurement of specific heat of large tissue samples up to boiling temperatures, and verify the method in phantom measurements.

2. Theory

The heat transfer equation when a sample with heat capacity c is heated by applying power with a mass-specific energy rate p (W kg^{-1}) is

$$c \frac{\partial T}{\partial t} = \frac{\nabla \cdot k \nabla T}{\rho} + p. \quad (1)$$

To measure temperature-dependent specific heat c , the temperature distribution inside the sample must be known so that the term describing thermal conduction (first term on right-hand side) is known. Furthermore, power density at a location where temperature is measured must be known.

We attempted to obtain uniform power density in a large sample with the set-up shown in figure 1. A cube-shaped sample with known dimensions and mass is placed between two plate electrodes. Under ideal conditions, this set-up produces uniform heating of the sample. The sample is thermally isolated so that no heat is lost, resulting in uniform temperature distribution in the sample, i.e., the thermal conduction term in equation (1) is zero. Under these conditions, we can obtain the specific heat of the sample by measuring the temperature at an arbitrary location:

$$c = \frac{P}{m \cdot (\partial T / \partial t)} \quad (2)$$

where P is the total power applied to the sample and m is the sample mass.

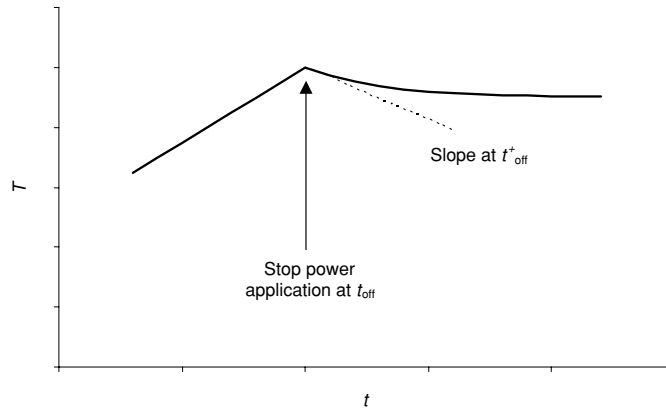


Figure 2. Typical temperature–time course. Power application is stopped at t_{off} . Slope after power shutdown is used to correct for error resulting from conductive losses.

The following assumptions are made:

- homogeneous sample,
- negligible heat loss to the environment,
- uniform contact between electrodes and sample surfaces,
- sample mass does not change (e.g., due to vaporization).

2.1. Correction for heat loss

From preliminary experiments, we found that at high temperatures (>50 °C) the heat conduction term was not negligible in our set-up; we observed a significant decline in temperature after power was turned off. One way to reduce this error would be to increase the width of the sample so that the temperature profile near the center is more homogeneous. However, we can also correct for this error using the following method. Figure 2 shows the temperature–time course during an experiment. The temperature rise during power application is almost linear, followed by a slow exponential decay after power is shut off at t_{off} . Since the temperature distribution is the same right before and after the power is turned off, the heat conduction term (see equation (1)) also has to be identical. The heat transfer equation right before t_{off} (i.e., t_{off}^-) is

$$c \frac{\partial T}{\partial t} \Big|_{t_{\text{off}}^-} = \frac{\nabla \cdot k \nabla T}{\rho} + p. \quad (3)$$

Right after t_{off} , no power is applied and equation (3) becomes

$$c \frac{\partial T}{\partial t} \Big|_{t_{\text{off}}^+} = \frac{\nabla \cdot k \nabla T}{\rho}. \quad (4)$$

In equations (3) and (4), the time derivatives of temperature $\partial T/\partial t$ right before and after t_{off} are the slopes of the temperature–time course (see figure 2), which we can obtain from the experiments. If the temperature decline after power shut down is significant, we can use equations (3) and (4) to correct for thermal conduction-related temperature changes; from these equations, we can calculate the specific heat according to

$$c = \frac{P}{m \cdot \left(\frac{\partial T}{\partial t} \Big|_{t_{\text{off}}^-} - \frac{\partial T}{\partial t} \Big|_{t_{\text{off}}^+} \right)}. \quad (5)$$

This equation is very similar to equation (2), except we introduced a correction term—the slope of the temperature decrease after power shut down. We can only obtain this correction term at temperatures where we turn the power off, so we can measure the slope of temperature decrease, i.e., we can only obtain the correction term at a number of distinct temperatures. To apply the correction for other temperatures within the measurement temperature range, we can interpolate the correction term between the distinct temperatures where it was measured.

The experimental procedure to determine specific heat is then:

- heat to temperature T_1 , and turn off power to determine slope of temperature decline
- heat to temperature T_2 , and turn off power to determine slope of temperature decline, and so on.

Thereby, we are able to directly measure specific heat of the sample, without need for calibration with a substance of known specific heat.

3. Methods

3.1. Numerical analysis

We used finite element method analysis to determine temperature distribution in a sample ($5 \times 5 \times 4 \text{ cm}^3$) insulated by a 1 cm layer of expanded polystyrene (see figure 1). Thermal and electrical properties of 0.4% saline (i.e., the properties of the phantom used in the experiments) were used for the sample. A constant power of 60 W was applied to the sample by application of a voltage difference across the sample (top to bottom in figure 1), until the temperature at the center reached 80 °C. A temperature of 25 °C was applied to the outer boundary of the model.

All simulations were performed using ABAQUS finite element software on a Sun Blade 1000 workstation with 2 GB of memory and 80 GB of hard disk space. The 3D model had $\sim 10\,000$ elements. Haemmerich *et al* (2002) describe the modeling procedure in more detail.

3.2. Experimental set-up

Figure 1 shows the experimental set-up. Our samples were made of 2.5% agar–water (mass fraction), and were prepared using a 0.4% saline solution (mass fraction) to provide an electrically conductive sample that can be heated by application of electric current. The specific heat of this sample is the same as that of water, and changes little with temperature; the salt only causes a slight change in specific heat compared to water; the specific heat of our sample is $c = 4160 \text{ J (kg K)}^{-1}$ at 25 °C, with a slight increase to $4178 \text{ J (kg K)}^{-1}$ at 80 °C (Incropera and DeWitt 1996). The sample was cut from an agar–water block with a surgical blade ($5 \times 5 \times 4 \text{ cm}^3$, measured with a standard ruler). The sample was placed between two plate electrodes ($5.0 \times 5.0 \text{ cm}^2$) made of sheet metal (Zn-plated Fe). A thin layer of conductive gel was applied to the electrodes to reduce errors from uneven sample surfaces that may result in uneven contact. The sample was thermally insulated by 1 cm thick expanded polystyrene ($k = 0.03 \text{ W (m K)}^{-1}$) on each side. We placed a weight of 200 g on top of this set-up to ensure electric contact between sample and electrodes. Six electrically insulated thermocouples (accuracy 0.2 °C) were placed in the center plane between the electrodes inside the sample as shown in figure 3. The temperature was recorded at 5 samples/s during the experiment.

A commercial generator was used to heat the sample (PDX-500, Advanced Energy) by applying electric current of 375 kHz with constant power to the sample. We applied 60 W (accuracy 2 W) of power to heat the sample, which resulted in a heating rate of $\sim 10 \text{ °C min}^{-1}$.

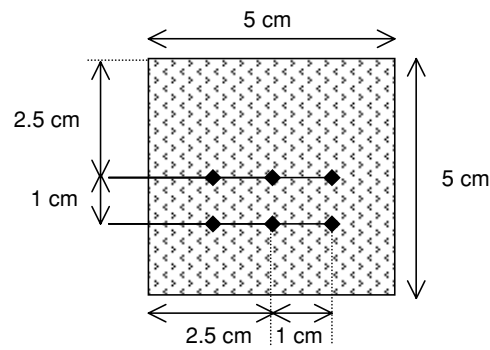


Figure 3. Sample (top view, center plane), with six thermocouple locations.

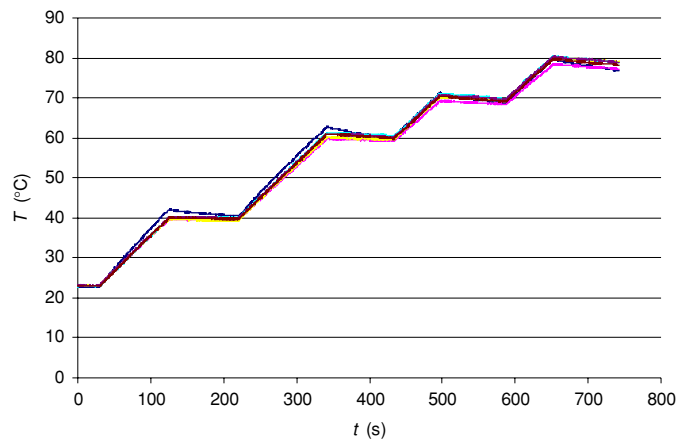


Figure 4. Typical temperature–time course of six temperatures measured by thermocouples during an experiment. Sample was heated to 40, 60, 70 and 80 °C, with intermittent 1.5 min cool-down cycles.

(This figure is in colour only in the electronic version)

To allow for correction as described above, we had to include cool-down cycles. Starting at room temperature (25 °C), we heated to 40, 60, 70 and 80 °C, with an intermittent 1.5 min cool-down cycle after each of the temperatures was reached. Before and after each experiment, we measured the mass of the sample with a scale (Ohaus CS-200, 0.1 g accuracy). Sample masses were between 85 and 100 g, and were reduced by ~2 g after the heating, possibly due to water loss.

3.3. Data evaluation

We calculated the initial slope of temperature decrease after power was turned off at 40, 60, 70 and 80 °C, to correct for errors caused by thermal conduction as described above. We used a linear approximation from these data points to correct for this error at all temperatures between 25 °C and 80 °C (see figure 4). We averaged the temperature of the six thermocouples, excluding up to two thermocouple readings that were outliers (i.e., difference was >5 °C compared to other temperatures). We determined the slope of temperature rise during heating; since this derivative is very sensitive to noise in the data, we used moving averages with a window size of 2 °C to reduce noise. We further measured the initial slope of temperature

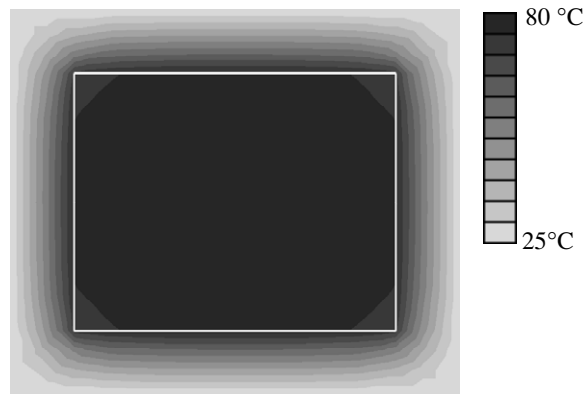


Figure 5. Temperature distribution in computer model. A sample (white rectangle) surrounded by styrofoam was heated to 80 °C by application of a voltage drop from top to bottom surface. The model confirms uniform heating of the sample.

decay after power shutdown. From these data we calculated the specific heat of the sample using equation (5) within our measurement temperature range of 25–80 °C. For the sample mass, we used the average of the mass before and after the heating, since the weight loss was comparably small, and we did not know at which temperature the mass loss occurred. We performed a total of eight experiments in four samples. For each experiment, we determined error versus temperature within the measurement temperature range. We then calculated average error at each temperature for our eight experiments, by comparing the value to the known specific heat of the sample.

4. Results and discussion

Figure 4 shows the temperature–time course measured by the six thermocouples during one of the experiments. There is very little deviation in the temperatures measured at the different sample locations, confirming uniform heating of the sample. Figure 4 also shows that temperature decrease during the cool-down cycle is noticeable as higher temperatures are reached. Figure 5 shows the temperature distribution of the computer model. The temperature is uniform except at the edges, confirming our assumption of uniform heating. Figure 6 shows the initial slope of temperature decay after power is turned off for the different temperatures of 40, 60, 70 and 80 °C; as the slope changes fairly linearly with temperature, we used a linear approximation to correct at all temperatures between 25 °C and 80 °C in equation (5); R^2 was between 0.96 and 0.99. Figure 7 shows the temperature-dependent specific heat c obtained in one of the experiments; results are shown both with correction for the error caused by thermal conduction using equation (5), and without correction using equation (2). The deviation between the two curves increases with higher temperatures, as sample cooling due to thermal conduction losses intensifies with temperature. The same is apparent in figure 8, which shows the measurement error at different temperatures, averaged over eight samples, with and without error correction. Figure 9 shows the temperature dependence of specific heat (Average \pm StdDev of eight experiments); the actual specific heat is represented by the dashed line. The error averaged over eight samples, and averaged over the measurement temperature range (25–80 °C) was $3.1 \pm 1.6\%$; due to the small change of specific heat of our sample with temperature ($\sim 0.3\%$ change between 25 °C and 80 °C), averaging between 25 °C and 80 °C

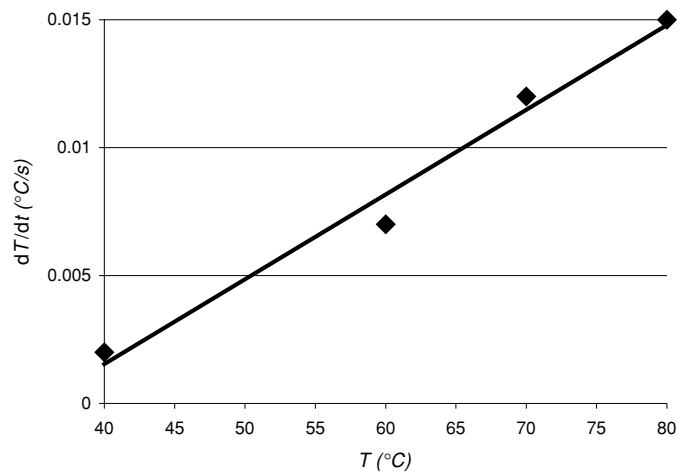


Figure 6. Initial slope of temperature decrease at 40, 60, 70 and 80 °C (diamonds), with linear approximation (line) (experiment #4). $R^2 = 0.98$.

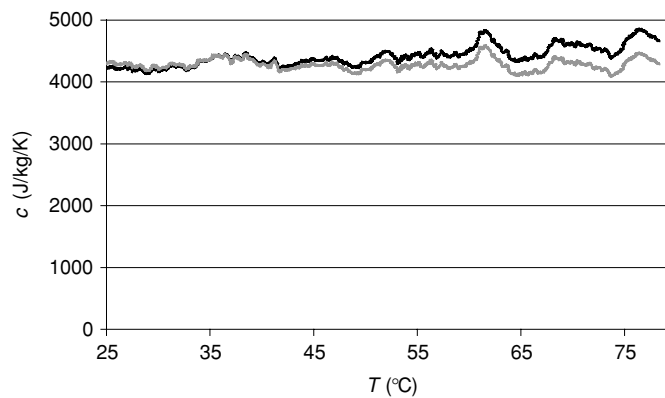


Figure 7. Measured specific heat with (gray), and without correction (black) (experiment #4). The actual specific heat of the sample was $4160 \text{ W (kg K)}^{-1}$.

is justified. Table 1 shows the measured values of specific heat for each experiment, including error averaged over the measurement temperature range.

The following are the sources contributing to the error:

- shape of the sample is not ideal,
- sample mass changes during the experiment,
- non-uniform contact between electrodes and sample due to uneven electrode and sample surfaces,
- measurement errors in temperature, applied power and sample mass,
- sample inhomogeneity (unlikely a factor with our agar–water sample, but may be important, e.g., in biological samples).

Temperature measurements at several locations allow reduced errors introduced by sample inhomogeneities. Larger sample dimensions reduce errors from deviations in sample shape, and non-uniform electrode–sample contact; the sample temperature can be measured farther away from electrodes where heating is more uniform than close to the electrodes.

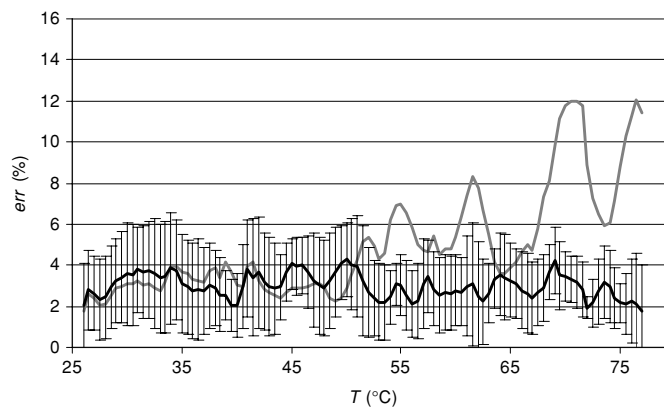


Figure 8. Error (average of eight experiments) with (black line, \pm StdDev) and without (gray line, \pm StdDev) correction.

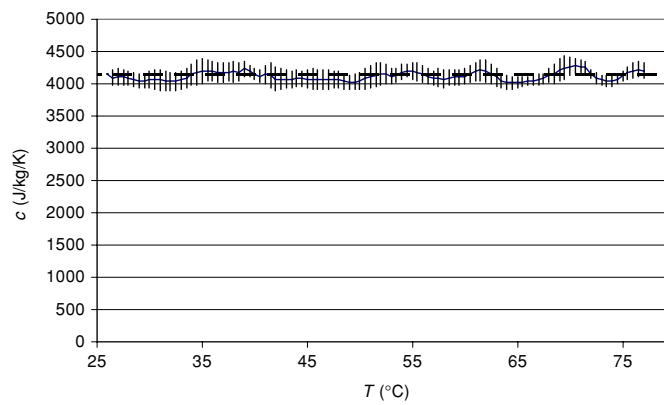


Figure 9. Specific heat (average of eight experiments, with StdDev). The actual specific heat is indicated by the dashed line.

Table 1. Average specific heat, average error and maximum error, averaged over measurement temperature range (25–80 °C), for each experiment.

Experiment #	c_{ave} (J kg ⁻¹ K ⁻¹)	Err _{ave} (%)	Err _{max} (%)
1	4279 \pm 107	3.4 \pm 2.5	9.5
2	3920 \pm 55	5.8 \pm 1.3	10.0
3	4125 \pm 105	2.2 \pm 1.5	7.7
4	4284 \pm 89	3.1 \pm 2.0	10.2
5	4149 \pm 98	2.0 \pm 1.2	6.9
6	4095 \pm 91	2.3 \pm 1.4	6.5
7	4140 \pm 81	1.7 \pm 1.1	5.7
8	3977 \pm 84	4.5 \pm 1.9	8.4
Ave	4121 \pm 89	3.1 \pm 1.6	8.1 \pm 1.7

Last line shows averages of eight experiments.

5. Conclusion

For biological materials, DSC is commonly used to determine temperature-dependent specific heat of biological materials. For DSC small samples are required, where errors may be introduced especially at high temperatures depending on sample sealing.

We present a simple instrument that allows measurement of temperature-dependent specific heat of large samples, and confirmed performance by measurements in phantoms. The average error was $3.1 \pm 1.6\%$, which is sufficient for measurement of biological tissues where the typical variability is in the range of 5–10%. The error may be larger for measurement of tissues due to inhomogeneities.

Acknowledgment

This study was supported by the National Institute of Health (NIH) under grant DK58839.

References

- Duck F A 1990 *Physical Properties of Tissue* (London: Academic) pp 167–223
- Haemmerich D, Tungjitkusolmun S, Staelin S T, Lee F T Jr, Mahvi D M and Webster J G 2002 Finite-element analysis of hepatic multiple probe radio-frequency ablation *IEEE Trans. Biomed. Eng.* **49** 836–42
- Incropera F P and DeWitt D P 1996 *Fundamentals of Heat and Mass Transfer* (New York: Wiley) pp 846–7
- Mohesnin N M 1980 *Thermal Properties of Food and Agricultural Materials* (New York: Gordon and Breach)
- Rahman S 1995 *Food Properties Handbook* (Boca Raton, FL: CRC Press)
- Ramachandran T, Sreenivasan K and Sivakumar R 1996 Water vaporization from heated tissue: an in vitro study by differential scanning calorimetry lasers *Surg. Med.* **19** 413–5
- Sweat V E 1986 *Thermal Properties of Foods* (New York: Dekker)
- Tang J, Sokhansanj S, Yannacopoulos S and Kasap S O 1991 Specific-heat capacity of lentil seeds by differential scanning calorimetry *Trans. ASAE* **34** 517–22
- Touloukian Y S and Buyco E H 1970 *Thermophysical Properties of Matter* (New York: IFI/Plenum)